Enhancement in thermoelectric power factor of M/T/N and M/Bi/M/Bi/M (M and N = Cu or Ni) composite devices welded with T = Bi or Bi$_{0.88}$Sb$_{0.12}$ alloy

OSAMU YAMASHITA, HIROTAKA ODAHARA, KOUJI SATOU
Faculty of Engineering, Ehime University, Bunkyocho, Matsuyama 790-8577, Japan
E-mail: yamashio@eng.ehime-u.ac.jp

The resultant thermoelectric power factors P of M/T/N and M/Bi/M/Bi/M (M and N = Cu or Ni) devices welded with T = Bi or Bi$_{0.88}$Sb$_{0.12}$ alloy were measured at 298 K and compared with P values calculated as a function of x by treating these devices as an electrical and thermal circuit, where x is the ratio of thickness of Bi or Bi-Sb alloy to the interval between two thermocouples. Consequently, the Seebeck coefficients α of M/T/N devices were enhanced significantly in the middle range from $x = 0.3$ to 0.8, and the observed P values have a local maximum at small x below $x = 0.35$. The x-dependence of P values of M/T/N devices was found to be explained well by the simple model proposed here when an enhancement factor in α and some reduction in thermal conductivity κ of pure metal were taken into the calculation. As a whole, however, the observed P values of double-layered M/Bi/M/Bi/M devices are lower than those of single-layered M/Bi/M, so that the macroscopic multi-layering of thermoelectric materials has no effect on the enhancement in P. The maximum P (=22.1 mW/K^{2}m) of Cu/Bi-Sb/Cu is 1.5 times larger than that of Cu/Bi/Cu and reached 3.6 times as large as the mean value of 5.7 and 6.6 mW/K^{2}m of the high-performance bulk p- and n-type bismuth-telluride compounds.
© *2005 Springer Science + Business Media, Inc.*

1. Introduction

In recent years there has been renewed interest in finding new materials and structures for use in highly efficient cooling and energy conversion systems [1, 2]. This interest has been stimulated in considerable part by the opportunities that quantum well and quantum wire superlattices [3–5] might result in thermoelectric materials with high power factors $P = \alpha^2/\rho$, where α is the Seebeck coefficient and ρ is the electrical resistivity. P is given in terms of the material's electrical transport properties, and it enters the thermoelectric figure of merit $Z = P/\kappa$, where κ is the total thermal conductivity which contains both lattice and electronic contributions. Thus, P provides a measure of the quality of a material for cooling [6].

Recently, the resultant P of two-component composite device was calculated by Bergman and Fel [7], who predicted that the resultant P can be sometimes be greater than the power factors of two different pure components, by employing the model based on the classical continuum linear transport theory. Most recently, such an enhancement in P of composite devices has been observed by the present authors using macroscopic M/Bi/N (M and N = Cu or Ni) devices [8].

Theoretically, the resultant maximum P is expected to increase significantly when Bi-Sb alloy with a thermal conductivity lower and a Seebeck coefficient higher than pure Bi was employed instead of pure Bi. The composite devices with a sandwich structure are thus considered as means of further increase in P of bulk thermoelectrics.

In this paper, the dependence of P values on the relative thickness of Bi or Bi-Sb alloy was investigated experimentally for macroscopic M/Bi/M/Bi/M and M/Bi-Sb/N composite devices. The resultant P of the composite device with a sandwich structure was calculated as a function of relative thickness of Bi or Bi-Sb alloy by treating it as an electrical and thermal circuit, and the calculation method is much simpler analytically than the model proposed by Bergman and Fel [7]. The observed P values were compared with the power factors calculated based on the model proposed here.

The purpose of this paper is to investigate to what degree the maximum P of single- and double-layered composite devices is increased by employing Bi-Sb alloy instead of pure Bi, and to demonstrate the validity of the model proposed here by comparing the observed P values with the calculated ones.
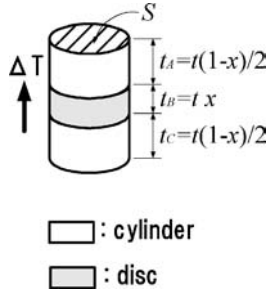
Figure 1 Composite thermoelectric device (CTD) with a sandwich structure (A/B/A) in which a disc of thermoelectric material B is sandwiched between two cylinders of materials A and C. The direction of the temperature gradient is along the cylindrical axis of the device.

2. Calculations and experiments
2.1. Calculations of electrical resistivity, Seebeck coefficient and power factor of a composite device

Let us consider a component composite thermoelectric device (CTD) with a sandwich structure (A/B/C) in which a disc of the thermoelectric material B is sandwiched between two cylinders composed of two different materials A and C, as shown in Fig. 1. Here, we calculate the resultant P for CTD by treating CTD as an electrical and thermal circuit, in which the direction of the temperature gradient is along the cylindrical axis. [8, 9] The materials A, B and C have the same cross-sectional area S and two different thicknesses $t_A = t_C$ and t_B, respectively. It was assumed here that the scattering of carriers and phonons never occurs at the interface between a disc and two cylinders. When α, κ and ρ of three materials A, B and C are denoted by α_A, α_B and α_C, κ_A, κ_B and κ_C and ρ_A, ρ_B and ρ_C, respectively, the total electrical resistivity ρ of CTD is expressed as

$$\rho = \frac{1}{t}(\rho_A t_A + \rho_B t_B + \rho_C t_C). \quad (1)$$

Here if we suppose $t_A = t_C = t(1-x)/2$ and $t_B = tx$, where t is the total thickness and x is the ratio of t_B of a disc to the total thickness t, Equation 1 can be rewritten as

$$\rho = \rho_B \left\{ x + \frac{(b_1 + b_2)(1-x)}{2} \right\}, \quad (2)$$

where $b_1 = \rho_A/\rho_B$ and $b_2 = \rho_C/\rho_B$. For a given temperature difference ΔT, the temperature difference generated in each thermoelectric should be proportional to thickness but inversely proportional to thermal conductivity, at least for a thin CTD. Taking this into account, the ratios of ΔT_A and ΔT_C to ΔT_B are expressed as

$$\frac{\Delta T_A}{\Delta T_B} = \frac{t_A \kappa_B}{t_B \kappa_A} = \frac{(1-x)}{2c_1 x} \quad (3)$$

and

$$\frac{\Delta T_C}{\Delta T_B} = \frac{t_C \kappa_B}{t_B \kappa_C} = \frac{(1-x)}{2c_2 x}, \quad (4)$$

where $c_1 = \kappa_A/\kappa_B$ and $c_2 = \kappa_C/\kappa_B$. The total temperature difference ΔT between both ends of CTD is given

by

$$\Delta T = \Delta T_A + \Delta T_B + \Delta T_C. \quad (5)$$

By substituting Equations 3 and 4 into Equation 5, the ratio of thermal difference ΔT_B generated in a sandwiched material B to the total thermal difference ΔT is expressed as

$$\frac{\Delta T_B}{\Delta T} = \frac{x}{c(1-x) + x}, \quad (6)$$

where $c = (c_1 + c_2)/2c_1 c_2$. The total thermal voltage ΔV generated by ΔT_A, ΔT_B and ΔT_C is written as

$$\Delta V = \Delta T_A \alpha_A + \Delta T_B \alpha_B + \Delta T_C \alpha_C. \quad (7)$$

Therefore, the overall Seebeck coefficient α is expressed as

$$\alpha = \frac{\Delta V}{\Delta T} = \alpha_B \frac{(1-x)(a_1 c_2 + a_2 c_1) + 2c_1 c_2 x}{(1-x)(c_1 + c_2) + 2c_1 c_2 x} \quad (8)$$

using Equations 3–7, where $a_1 = \alpha_A/\alpha_B$ and $a_2 = \alpha_C/\alpha_B$. Substituting Equations 2 and 8 into the equation $P = \alpha^2/\rho$, the resultant P is expressed using P_B of the thermoelectric material as

$$\frac{P}{P_B} = \left\{ \frac{(1-x)(a_1 c_2 + a_2 c_1) + 2c_1 c_2 x}{(1-x)(c_1 + c_2) + 2c_1 c_2 x} \right\}^2$$
$$\times \frac{2}{2x + (b_1 + b_2)(1-x)}, \quad (9)$$

where $P_B = \alpha_B^2/\rho_B$. Of course, Equation 9 reduces to $P = P_B$ if $x = 1$ and to $P = P_A = P_C$ if $x = 0$ and A = C. It may be verified by a simple analysis that when P_B is larger than P_A and P_C, the condition necessary for making P/P_B larger than 1 is expressed as

$$\left(\frac{1}{a} \frac{1}{c} \frac{(1-b)}{2} \right) \gg (c - a), \quad (10)$$

where $a = (a_1 c_2 + a_2 c_1)/2c_1 c_2$ and $b = (b_1 + b_2)/2$. Therefore, P/P_B can have a local maximum greater than its maximum among the three different pure components, as long as this condition is satisfied. Further increase in c_1 and c_2 and further decrease in a_1 and a_2 make it easier to satisfy the inequality of Equation 10. In other words, it means that the resultant maximum P should increase significantly as the ratio of the thermal conductivity of a metal with a low electrical resistivity to that of a thermoelectric material with a high Seebeck coefficient becomes large. For a composite device composed of two different types of materials, it was suggested by Bergman and Fel [7] that the power factor should be enhanced markedly at an optimum volume fraction. However, the same was also demonstrated theoretically by using the simple model that the power factor of sandwiched composite devices can be enhanced significantly, even in the composite device composed of three different types of materials.

2.2. Sample preparation

The M/T/N and M/Bi/M/Bi/M (M and N = Cu or Ni and T = Bi or $Bi_{0.88}Sb_{0.12}$) composite devices were prepared by the welding method, using Cu and Ni of 99.9% and Bi and Sb of 99.99%, which have cylindrical shapes with a diameter slightly smaller than 5 mm. The cylindrical ingots of Bi and Bi-Sb alloy were prepared by melting in an evacuated glass tube of an inner diameter slightly smaller than 5 mm by an induction heating to make a homogeneous melt without segregation. Of course, all of these composite devices satisfy the inequality of Equation 10. The thickness of each metal was determined so that Bi and Bi-Sb alloy sandwiched between these metals have various thicknesses but the total length of composite devices becomes 20 mm. The welded M/Bi/M/Bi/M devices were fabricated so that two sandwiched Bi discs have almost the same thickness. After both end surfaces of all cylindrical metals were polished mechanically by the lapping method to make flat the welded surface, a set of cylindrical metals and Bi or Bi-Sb alloy was put in a glass tube of an inner diameter φ5 mm so that they are sandwiched between two metals in a glass tube. Since Bi and $Bi_{0.88}Sb_{0.12}$ have very low melting points of 544 and 598 K [10], as compared to those of Cu and Ni, Bi and Bi-Sb alloy were first melted in a glass tube by an induction heating. While Bi or Bi-Sb alloy is melted, cylindrical metals were welded by compacting two metallic cylinders of both ends at a constant force of 2 N using two iron rods, as shown in Fig. 2. After a welded cylinder was naturally cooled to room temperature, it was ejected out of a glass tube using an iron rod. Two photographs of two types of devices are shown in Fig. 3a and b. The thickness t_B of Bi and Bi-Sb alloy was measured by polishing the surface along the cylindrical axis of a welded device, so that the boundary between metal and Bi or Bi-Sb alloy becomes clear, as shown in Fig. 3c. After polishing, no crack and no exfoliation were detected at the boundaries of all devices. Then the average grain sizes of Bi and B-Sb alloy were approximately 70 and 100 μm, respectively, which remained almost unchanged before and after welding.

All of the composite devices were subjected to Seebeck coefficient and electrical resistivity measurements (Sinku-Riko, Inc., Model ZEM-1). The Seebeck coefficient α was measured by the conventional technique, using two alumel-chromel thermocouples set at an interval of 8 mm, in the temperature range from 293 to 303 K with the temperature difference of about 10 K.
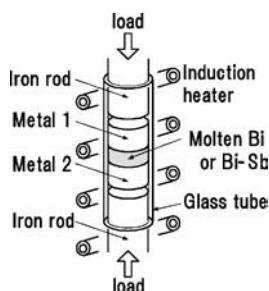

Figure 2 Fabrication method of composite devices welded with Bi or $Bi_{0.88}Sb_{0.12}$ alloy.
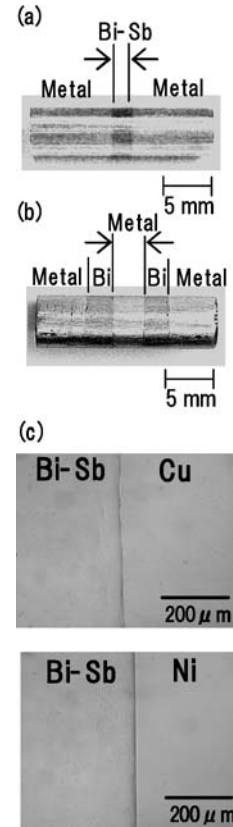

Figure 3 Photographs of welded thermoelectric devices of Cu/Bi-Sb/Cu (a) and Cu/Bi/Cu/Bi/Cu (b) and two boundaries welded with $Bi_{0.88}Sb_{0.12}$ alloy (b).

The composite devices were then adjusted so that two metals of both ends have the same length between two thermocouples. The electrical resistivity ρ was measured concurrently by the four-probe method. All of these measurements were performed along the cylindrical axis.

In order to observe whether the c axis of the welded Bi and Bi-Sb alloy is aligned along the cylindrical axis of the device, Bi and Bi-Sb alloy before and after welding were investigated by X-ray diffraction (XRD) using Cu-K_α radiation ($\lambda = 1.5418$ Å).

3. Results and discussion
3.1. Dependence of the resultant ρ, α and P on relative thickness x of Bi

The resultants ρ and α of M/Bi/N and M/Bi/M/Bi/M (M, N = Cu or Ni) composite devices were measured at 298 K as a function of x, where x is the ratio of thickness of Bi to an interval of 8 mm. No significant difference in ρ and α occurred in any device when the direction of the temperature gradient was reversed. The measured ρ values (see Table I) of pure Cu, Ni and Bi are in good agreement with the previous data [11, 12]. Moreover, the experimental α values of Bi before welding is very close to -68.3 μ V/K calculated as the mean value using the equation $\alpha = (\alpha_{33} + 2\alpha_{11})/3$, where α_{33} and α_{11} were Seebeck coefficients measured at 300 K along the trigonal and binary directions of single-crystal Bi. [12].

As shown in Fig. 4, the observed ρ values of M/Bi/N and M/Bi/M/Bi/M (M and N = Cu or Ni) devices

TABLE I Electrical resistivities and Seebeck coefficients measured at 298 K for pure Cu, Ni, Bi and $Bi_{0.88}Sb_{0.12}$ cylindrical rods with a length of 20 mm and a diameter of φ 5 mm

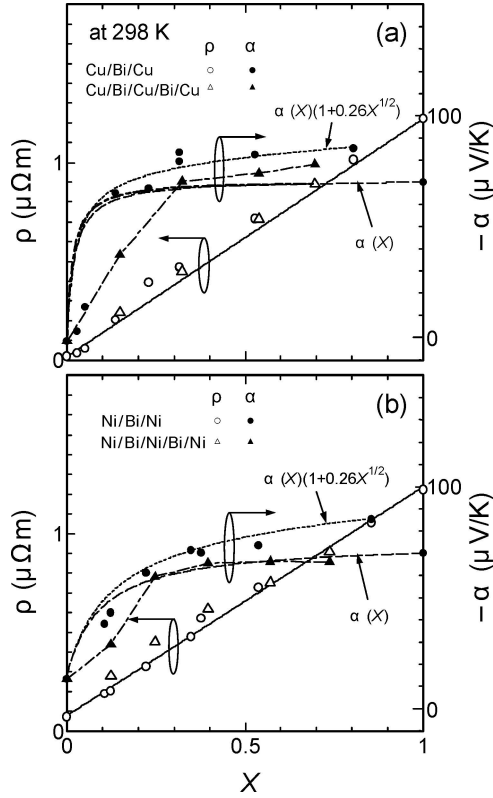|		Cu	Ni	Bi	$Bi_{0.88}Sb_{0.12}$
Electrical resistivity	ρ ($\mu\Omega$m)	0.0171	0.0720	1.222	1.700
Seebeck coefficient	α (μV/K)	+1.9	−15	−70	−85
Thermal conductivity	κ (W/mK)	401[a]	91[a]	7.9[b]	4.9[b]
Power factor	P (mW/K^{2}m)	0.21	3.13	4.01	4.25
Figure of merit	ZT	1.57×10^{-4}	1.02×10^{-2}	0.15	0.26

[a] Ref. 11.
[b] Ref. 16.

Figure 4 Resultants ρ and α as a function of x for thermoelectric devices of Cu/Bi/Cu and Cu/Bi/Cu/Bi/Cu (a) and Ni/Bi-Sb/Ni and Ni/Bi/Ni/Bi/Ni (b) welded with pure Bi. The solid and dashed curves denote $\rho(x)$ and $\alpha(x)$ calculated from Equations 1 and 8 for Cu/Bi/Cu and Ni/Bi/Ni devices, respectively, where the experimental values are listed in Table I. The dotted curves are obtained by multiplying the dashed curves $\alpha(x)$ by a factor of $(1 + 0.26x^{1/2})$, so as to reproduce well the observed α values.

increase linearly with an increase of x and fall roughly on the solid curves $\rho(x)$ calculated from Equation 1 using the experimental values, as listed in Table I. In contrast, the observed α values of M/Bi/M devices increase *abruptly* with an increase of x and tend to saturate to −85 μ V/K at $x \doteq 0.8$, while those of M/Bi/M/Bi/M increase *slowly* with an increase of x and at $x = 0.2$–0.3 tend to approach the dashed curves $\alpha(x)$ calculated from Equation 8 using the experimental values, as listed in Table I. However, the observed α values of double-layered M/Bi/M/Bi/M devices are much lower than the solid curve below $x = 0.3$. To the contrary, the observed α values of single-layered M/Bi/M devices are 10–20% higher than the dashed curves $\alpha(x)$ in the middle region from $x = 0.3$ to 0.8, but they agreed well with the dotted curves obtained by multiplying the dashed curves $\alpha(x)$ by an enhancement factor of $(1 + 0.26x^{1/2})$. The max-

imum α values of M/Bi/M devices are 21% higher in absolute value than −70 μ V/K of pure Bi. However, such a significant enhancement in α is scarcely seen in M/Bi/M/Bi/M devices. It indicates that the electron scattering effect never appears in such multi-layered composite devices of bulk materials, unlike superlattice systems [13]. As well-known, α of pure Bi has a strong anisotropy, that is, α_{33} is just twice as large as α_{11}. Whether or not α is enhanced after welding, therefore, should depend on the difference in the degree of alignment of the c axis of welded Bi. For this reason, XRD measurement was made on Bi-Sb alloy powder pulverized before welding and on the cross-section of cylindrical Bi and Bi-Sb alloy ($x = 0.5$ to 0.8) before and after welding, as shown in Fig. 5. However, there was no significant difference between their XRD patterns in any device, so that Bi and Bi-Sb alloy were an isotropic polycrystalline. Thus, it is not clear at present that the reason why α of M/Bi/M devices was enhanced significantly in the region from $x = 0.5$ to 0.8.

The resultant P was plotted as function of x for M/Bi/M and M/Bi/M/Bi/M devices in Fig. 6. The observed P values have a local maximum at $x = 0.2$—0.35 in any device. The solid curves denote P values calculated from Equation (9) using the experimental values, as listed in Table I. Particularly in Cu/Bi/Cu device, the observed maximum P at $x \doteq 0.3$ is much lower than the calculated maximum P at $x \doteq 0.04$, as shown in Fig. 6a. This significant difference between the observed and calculated values may be attributed to
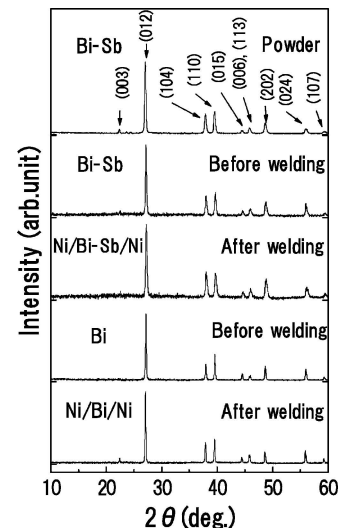

Figure 5 X ray diffraction patterns of Bi-Sb alloy powder pulverized before welding and cylindrical Bi and Bi-Sb alloy before and after welding.
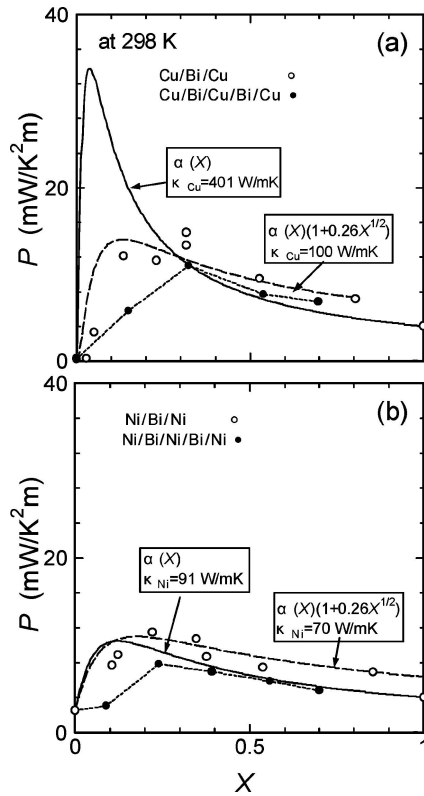
Figure 6 Resultant *P* as a function of *x* for thermoelectric devices of Cu/Bi/Cu and Cu/Bi/Cu/Bi/Cu (a), Ni/Bi/Ni and Ni/Bi/Ni/Bi/Ni (b) welded with pure Bi. The solid curves denote *P* values calculated from Equation 9 for Cu/Bi/Cu and Ni/Bi/Ni devices, where the experimental values used here are listed in Table I. The dashed curves are calculated using $\alpha(x)(1+0.26x^{1/2})$ and the thermoelectric properties of component materials, assuming that κ_{Cu} and κ_{Ni} are 100 and 70 W/mK, respectively.

an oversimplified model which holds exactly for a thin CTD alone. The reason is considered as follows. As Cu has a high thermal conductivity κ_{Cu} of 401 W/mK much larger than 7.9 W/mK of Bi, a relatively long Cu cylinder (corresponding to small *x*) is apt to generate the thermal radiation during the thermal conduction through a device, so that κ_{Cu} is reduced apparently to make small the difference between κ_{Cu} and κ_{Ni}. As evidence, it is supported by the fact that the dashed curve calculated using both a low κ_{Cu} of 100 W/mK and an enhanced Seebeck coefficient of $\alpha(x)(1 + 0.26x^{1/2})$, has a local maximum at larger *x* and further reproduces the experimental values precisely. Furthermore, as shown in Fig. 6b, in the small *x* region below *x* = 0.2, the observed *P* values of Ni/Bi/Ni are much closer to the solid curve than those of Cu/Bi/Cu, although an enhancement in α and a reduction in κ_{Ni} were not taken into the solid curve. The reason that the observed *P* of Ni/Bi/Ni approached the solid curve (without any correction) comes from a low κ_{Ni}, which is only 23% of κ_{Cu}. When an enhancement factor in α and a substantial reduction in κ of pure metal were taken into the calculation, the observed *P* of Ni/Bi/Ni coincided more closely with the calculated (dashed) curve. The maximum *P* (=14.8 mW/K²m) at *x* ≒ 0.3 of Cu/Bi/Cu device reaches 2.4 times as large as the mean value of 5.7 and 6.6 mW/K²m of the high-performance bulk *p*- and *n*-type bismuth-telluride compounds [14, 15]. However, such an increase in *P* never results in an in-

crease in *ZT*, because the resultant κ is expected to increase abruptly with increasing *x* in this region.

In M/Bi/M/Bi/M devices, the observed *P* values below *x* = 0.3 are much lower than the solid curves, while above *x* = 0.3 they fall roughly on the solid curves. The lowering of *P* values below *x* = 0.3 arises predominantly from the decrease in α and the agreement between the observed *P* values and the solid curves above *x* = 0.3 is owing to no or a little enhancement in α. Thus, *P* values of double-layered M/Bi/M/Bi/M devices never exceeded those of single-layered M/Bi/M, so that the macroscopic multi-layering of thermoelectric materials has no effect on the enhancement in *P*.

3.2. Dependence of the resultant ρ, α and *P* on relative thickness *x* of $Bi_{0.88}Sb_{0.12}$

Since the macroscopic double-layering of pure Bi was not effective to enhance the resultant *P* of composite devices, the devices composed of pure Cu and/or Ni and Bi-Sb alloy were limited to a single-layered device. Theoretically, the resultant *P* is expected to increase significantly when Bi-Sb alloy with a thermal conductivity lower and a Seebeck coefficient higher than pure Bi was employed instead of pure Bi. Similar to M/Bi/M devices, the resultants ρ and α of M/Bi-Sb/N (M and N = Cu or Ni) devices were measured at 298 K as a function of *x*. The measured ρ values (see Table I) of $Bi_{0.88}Sb_{0.12}$ alloy before welding is 12.8% higher than the previous data [12]. However, the experimental α value of $Bi_{0.88}Sb_{0.12}$ alloy coincides closely with -84.9 μV/K calculated as an average value using α_{33} (= -86.7 μV/K) and α_{11} (= -83.1 μV/K) measured at 300 K along the trigonal and binary directions of single-crystal $Bi_{0.88}Sb_{0.12}$ [12]. Since α of single-crystal $Bi_{0.88}Sb_{0.12}$ alloy has little anisotropy, α of $Bi_{0.88}Sb_{0.12}$ alloy hardly depends on whether or not the welded Bi-Sb alloy is an isotropic polycrystalline.

As shown in Fig. 7, the observed ρ values of M/Bi-Sb/N (M and N = Cu or Ni) devices increase linearly with an increase of *x* and fall closely on the solid curves ρ (*x*) calculated similarly to M/Bi/M devices. The observed α values of M/Bi-Sb/M devices increase abruptly with an increase of *x*, like M/Bi/M devices, and tend to saturate to -105 μ V/K at *x* ≒ 0.8. The observed α values of M/Bi-Sb/M devices exhibit *x*-dependences similar to those of M/Bi/M and coincided with the dotted curves corrected using the same enhancement factor as that of M/Bi/M devices. The maximum α (= -110 μV/K) values of M/Bi-Sb/M (M = Cu and Ni) devices are 29% higher in absolute value than -85 μV/K of $Bi_{0.88}Sb_{0.12}$ alloy, whose rate of increase is larger than 21% of M/Bi/M devices. From the fact that α of $Bi_{0.88}Sb_{0.12}$ has little anisotropy, as mentioned above, it is clear that the enhancement in α after welding has nothing to do with the degree of alignment of the *c* axis of welded $Bi_{0.88}Sb_{0.12}$ alloy. At present, thus, we cannot find any reason for such a significant enhancement in α in single-layered composite devices. In future, however, it would be necessary to clarify the mechanism of a significant enhancement in α, in order to obtain a higher thermoelectric power factor in macroscopic composite devices.
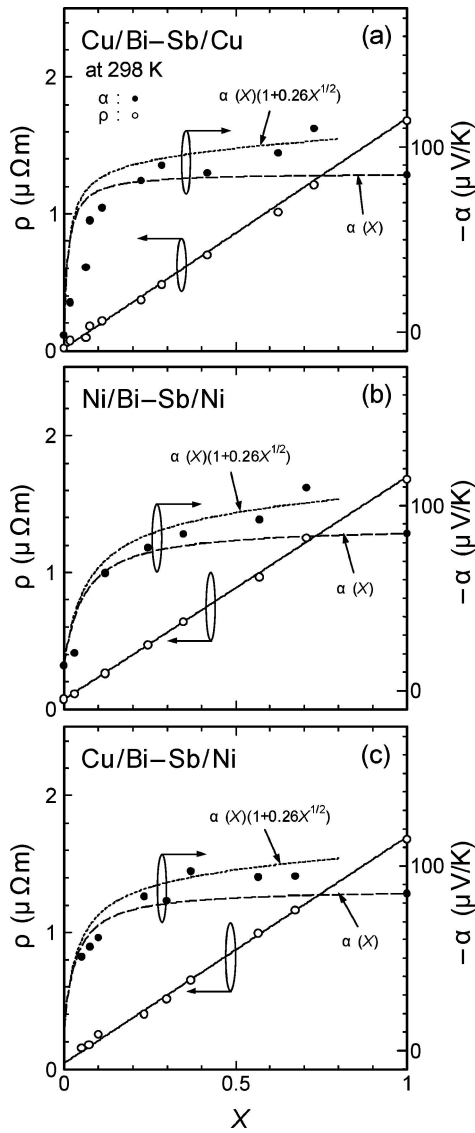
Figure 7 Resultants ρ and α as a function of x for thermoelectric devices of Cu/Bi-Sb/Cu (a), Ni/Bi-Sb/Ni (b) and Cu/Bi-Sb/Ni (c) welded with $Bi_{0.88}Sb_{0.12}$ alloy. The solid and dashed curves denote $\rho(x)$ and $\alpha(x)$ calculated from Equations 1 and 8, respectively, where the experimental values used here are listed in Table I. The dotted curves are obtained by multiplying the dashed curves $\alpha(x)$ by a factor of $(1 + 0.26x^{1/2})$, so as to reproduce well the observed α values.

Figure 8 Resultant P as a function of x for thermoelectric devices of Cu/Bi-Sb/Cu (a), Ni/Bi-Sb/Ni (b) and Cu/Bi-Sb/Ni (c) welded with $Bi_{0.88}Sb_{0.12}$ alloy. The solid curves denote P values calculated from Equation 9, using the experimental values, as listed in Table I. The dashed curves for devices (a)–(c) are calculated using $\alpha(x)(1 + 0.26x^{1/2})$ and the thermoelectric properties of component materials, assuming that κ_{Cu} values of devices (a) and (c) are 100 and 200 W/mK, respectively, and κ_{Ni} values of devices (b) and (c) are 45 and 68 W/mK, respectively.

The resultant P was plotted as a function of x for M/Bi-Sb/M devices in Fig. 8. As expected theoretically, the observed P values of M/Bi-Sb/M devices are higher than those of M/Bi/M and have a local maximum at $x = 0.06$–0.15. The x-values giving a maximum of M/Bi-Sb/M are less than half of those of M/Bi/M. The maximum P ($=22.1$ mW/K^{2}m) of Cu/Bi-Sb/Cu is 1.5 times larger than that of Cu/Bi/Cu and reached 3.6 times as large as the mean value of 5.7 and 6.6 mW/K^{2}m of the high- performance bulk p- and n-type bismuth-telluride compounds [14, 15]. An enhancement in the maximum P and a lowering of x-values giving a maximum P are attributed to a low κ_{Bi-Sb} which corresponds to 62% of that of pure Bi. In Cu/Bi-Sb/Cu devices, the observed P values below $x = 0.2$ are much lower than the solid curve, while above $x = 0.2$ the observed P values are slightly larger than the solid curve. However, below $x = 0.2$ the observed P values of Ni/Bi-Sb/Ni and Cu/Bi-Sb/Ni devices are much closer to the solid
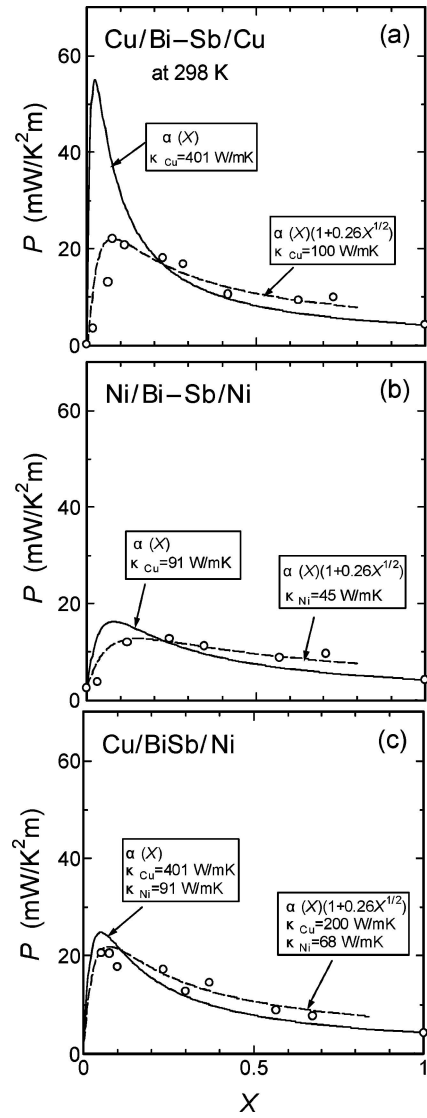
curve than those of Cu/Bi-Sb/Cu, while above $x = 0.2$ they exhibit tendencies very similar to those of Cu/Bi-Sb/Cu. When an enhancement factor of $(1 + 0.26x^{1/2})$ in α and some reduction in κ of pure metal were taken into the calculation, however, the observed P values of M/Bi-Sb/M coincide more closely with the calculated (dashed) curves than those of M/Bi/M. This better agreement in M/Bi-Sb/M devices is attributed to a lower κ_{Bi-Sb} of 4.9 W/mK. Therefore, the x-dependence of P values in M/Bi-Sb/M devices is also found to be explained well by the simple model proposed here, at least when an enhancement factor in α and some reduction in κ of pure metal were taken into account.

Next, let us consider by what factors the resultant P of a composite device is enhanced significantly. As shown in Fig. 9, the ratio of the temperature difference ΔT_B generated in a sandwiched Bi-Sb alloy to the total temperature difference ΔT increases abruptly with
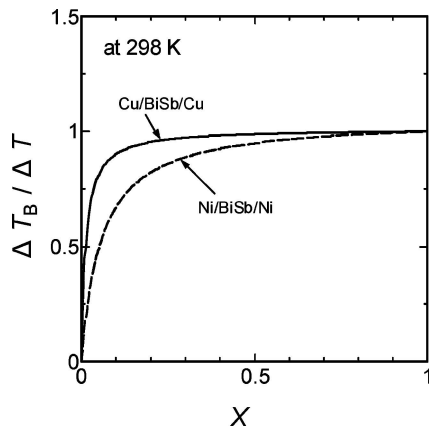
Figure 9 Ratio of thermal difference ΔT_B generated in a sandwiched thermoelectric disc to total thermal difference ΔT calculated using Equation 6 as a function of x for Cu/BiSb/Cu, Ni/BiSb/Ni and Cu/BiSb/Ni welded with $Bi_{0.88}Sb_{0.12}$ alloy, where the experimental values used here are listed in Table I.

increasing x and saturates to about 1 at $x = 0.2$ in Cu/Bi-Sb/Cu and at $x = 0.6$ in Ni/Bi-Sb/Ni. Taking into account that Cu has a higher κ than Ni, it is found that ΔT_B tends to saturate at smaller x as the ratio of the thermal conductivity of a metal to that of a thermoelectric material increases. In a word, the increase in the thermal conductivity of a metal increases the volume fraction of a metal in a device, resulting in the lowering of the total electrical resistivity. When the ratio of the thermal conductivity of a metal with a low electrical resistivity to that of a thermoelectric material with a high Seebeck coefficient is extremely large, therefore, a surprisingly high power factor is expected to be obtained by sandwiching a relatively thin thermoelectric disc between two metals.

4. Summary and conclusion
The resultant thermoelectric power factors P of sandwiched M/T/N and M/Bi/M/Bi/M (M and N = Cu or Ni and T = Bi or $Bi_{0.88}Sb_{0.12}$) devices were measured at 298 K and compared with P values calculated as a function of relative thickness x of Bi or Bi-Sb alloy by treating a device as an electrical and thermal circuit. The Seebeck coefficients of M/T/N devices were enhanced significantly in the middle range from $x = 0.3$ to 0.8, and the observed P values have a local maximum at small x below $x = 0.35$. The x-dependence of P values of M/T/N devices was found to be explained

well by the simple model proposed in this paper when an enhancement factor in α and some reduction in κ of pure metal were taken into the calculation. However, the observed P values of double-layered M/Bi/M/Bi/M devices are wholly lower than those of single-layered M/Bi/M, so that the macroscopic multi-layering of thermoelectric materials has no effect on the enhancement in P. The maximum P (=22.1 mW/K^{2}m) of Cu/Bi-Sb/Cu device is 1.5 times larger than that of Cu/Bi/Cu and reached 3.6 times as large as the mean value of 5.7 and 6.6 mW/K^{2}m of the high-performance bulk p- and n-type bismuth-telluride compounds.

When the ratio of the thermal conductivity of a metal with a low electrical resistivity to that of a thermoelectric material with a high Seebeck coefficient is large larger than the ratio of Cu/Bi-Sb/Cu device, an extremely high power factor would be obtained by sandwiching a relatively thin thermoelectric disc between two metals.

References
1. C. WOOD, *Prog. Phys.* **51** (1988) 459.
2. G. MAHAN, B. SALES and J. SHARP, *Phys. Today* **50** (1997) 42.
3. L. D. HICKS and M. S. DRESSELHAUS, *Phys. Rev. B* **47** (1993) 12727.
4. L. D. HICKS, T. C. HARMAN and M. S. DRESSELHAUS, *Appl. Phys. Lett.* **63** (1993) 3230.
5. D. A. BROIDO and T. L. REINECKE, *ibid.* **67** (1995) 1170.
6. H. J. GOLDSMID, "Thermoelectric Refrigeration" (Plenum, New York, 1964).
7. D. J. BERGMAN and L. G. FEL, *J. Appl. Phys.* **85** (1999) 8205.
8. H. ODAHARA, O. YAMASHITA, K. SATOU, S. TOMIYOSHI, J. TANI and H. KIDO, submitted to *J. Appl. Phys.*
9. O. YAMASHITA and H. ODAHARA, submitted to *J. Mater. Sci.*
10. B. LENOIR, A. DEMOUGE, D. PERRIN, H. SCHERRER, S. SCHERRER, M. CASSART and J. P. MICHENAUD, *J. Phys. Chem. Solids* **56** (1995) 99.
11. C. KITTEL, "Introduction to Solid State Physics" (John Wiley & Sons, New York, 1996).
12. W. M. YIM and A. AMITH, *Solid State Electrons* **15** (1972) 1141.
13. R. VENKATASUBRAMANIAN, E. SIIVOLA, T. COLPITTS and B. O'QUINN, *Nature* **413** (2001) 597.
14. O. YAMASHITA and S. TOMIYOSHI, *Jpn. J. Appl. Phys.* **42** (2003) 492.
15. *Idem., J. Appl. Phys.* **95** (2004) 6277.
16. *Idem., ibid.* **92** (2002) 3794.